

RESEARCH LETTER

10.1002/2017GL076045

Key Points:

- The timescales and 3-D structure of Circumpolar Deep Water (CDW) upwelling are missing from the zonally integrated overturning framework
- Lagrangian transit times of upwelling CDW are longer with coarser grid spacing or longer temporal averaging of the sampled velocity field
- As horizontal model resolution increases, particles complete fewer circumpolar loops thereby limiting interbasin merging of CDW

Supporting Information:

- Supporting Information S1
- Movie S1

Correspondence to:

H. F. Drake,
hdrake@mit.edu

Citation:

Drake, H. F., Morrison, A. K., Griffies, S. M., Sarmiento, J. L., Weijer, W., & Gray, A. R. (2018). Lagrangian timescales of Southern Ocean upwelling in a hierarchy of model resolutions. *Geophysical Research Letters*, 45, 891–898. <https://doi.org/10.1002/2017GL076045>

Received 8 AUG 2017

Accepted 11 JAN 2018

Accepted article online 22 JAN 2018

Published online 31 JAN 2018

Lagrangian Timescales of Southern Ocean Upwelling in a Hierarchy of Model Resolutions

Henri F. Drake^{1,2} , Adele K. Morrison^{1,3} , Stephen M. Griffies^{1,4} , Jorge L. Sarmiento¹ , Wilbert Weijer⁵, and Alison R. Gray^{1,6} 

¹Department of Atmospheric and Oceanic Sciences, Princeton University, Princeton, NJ, USA, ²Now at Massachusetts Institute of Technology and Woods Hole Oceanographic Institution Joint Program in Oceanography, Cambridge, MA, USA, ³Now at Research School of Earth Sciences, Australian National University, Canberra, ACT, Australia, ⁴NOAA/Geophysical Fluid Dynamics Laboratory, Princeton, NJ, USA, ⁵Los Alamos National Laboratory, Los Alamos, NM, USA, ⁶Now at School of Oceanography, University of Washington, Seattle, WA, USA

Abstract In this paper we study upwelling pathways and timescales of Circumpolar Deep Water (CDW) in a hierarchy of models using a Lagrangian particle tracking method. Lagrangian timescales of CDW upwelling decrease from 87 years to 31 years to 17 years as the ocean resolution is refined from 1° to 0.25° to 0.1°. We attribute some of the differences in timescale to the strength of the eddy fields, as demonstrated by temporally degrading high-resolution model velocity fields. Consistent with the timescale dependence, we find that an average Lagrangian particle completes 3.2 circumpolar loops in the 1° model in comparison to 0.9 loops in the 0.1° model. These differences suggest that advective timescales and thus interbasin merging of upwelling CDW may be overestimated by coarse-resolution models, potentially affecting the skill of centennial scale climate change projections.

Plain Language Summary In this paper we use a variety of ocean models to investigate how long it takes for deep ocean waters to upwell to the surface of the Southern Ocean around Antarctica. We track virtual particles in our simulated currents and show how they spiral southward and upward toward the surface. We find that this journey takes 87 years in a standard coarse-resolution climate model but only 17 years in a state of the art high-resolution climate model. We argue that the difference between the models is due to vortices which vigorously upwell the virtual particles but are too small to be represented in standard climate models. Particles also only loop around Antarctica 0.9 times in the high-resolution model compared to 3.2 times in the coarse-resolution model, suggesting that different kinds of upwelling waters have less time to mix with each other in coarse-resolution models. These differences in timescale and the number of loops suggest that there exist biases in long-term climate change projections using standard coarse-resolution climate models.

1. Introduction

The upwelling limb of the Southern Ocean meridional overturning circulation is responsible for absorbing anthropogenic heat and carbon in the climate system, as well as providing nutrients that sustain three quarters of the global ocean's biological productivity (Morrison et al., 2015). Understanding this upwelling has been challenging due to the extreme conditions in the Southern Ocean and the computational limitations in modeling mesoscale and submesoscale eddies (Marshall & Speer, 2012). Above major topographic obstacles (where the zonal mean of zonal pressure gradients vanish), southward eddy advection affects the upwelling in two distinct ways. Near the surface, eddy transport opposes the northward Ekman transport and hence reduces the upwelling. At depth, however, eddies are the primary mechanism driving the flow southward and upward along isopycnals. Although our understanding of Southern Ocean overturning is generally limited to a two-dimensional (latitude-density) framework, some studies have investigated the three-dimensional structure of the upwelling pathways (Döös, 1995; Döös et al., 2008; Tamsitt et al., 2017) and the importance of hotspots of cross-frontal eddy transport, primarily associated with topographic features (Dufour et al., 2015; Thompson & Sallée, 2012).

Upwelling timescales influence air-sea tracer fluxes and impact the transient climate response in the Southern Ocean (Armour et al., 2016). The timescale of the upwelling branch in the Southern Ocean is particularly difficult

to determine from observations because typical proxies for water age are not applicable to the upwelling limb of the Southern Ocean. Chlorofluorocarbons, which have atmospheric sources from the middle twentieth century, have not yet been detected in North Atlantic Deep Water in the Southern Ocean (Garzoli et al., 2015). Radiocarbon measurements are similarly difficult to interpret in the Southern Ocean due to the sparsity of data, large uncertainties, and the superposition of signals from northern- and southern-sourced waters (Khaliwala et al., 2012). Model estimates of the upwelling timescale have been limited to volume transport analysis in noneddy or time-averaged eddy models until very recently, with previous transit time estimates of 140 years (Iudicone et al., 2008) and 240 years (Döös, 1995) from 30°S and 25°S to the surface, respectively. Tamsitt et al. (2017) find relatively shorter timescales of 28–81 years across three different eddy models, with an 81 year timescale in a 1/6° model and a 28 year timescale in a different 0.1° model. While Tamsitt et al. (2017) hypothesize that these differences in timescales are due to differences in model resolution, they may also be due to a number of other model differences. Recent efforts aimed at improving eddy parameterizations in noneddy models have focused primarily on zonally integrated transport (in particular, the response of transport to wind stress) (Gent, 2016). Little is known about upwelling either transit times in eddy models or the effects of eddies on these timescales.

Using a suite of climate models with ocean resolutions of 1°, 0.25°, and 0.1°, along with a Lagrangian analysis tool, we track Lagrangian particles released at depth at 30°S until they reach the upper layers of the Southern Ocean. We calculate transport-weighted pathways for seawater and the corresponding timescales of upwelling and find a strong dependence on model resolution. We hypothesize that the dependence is caused by differences in mesoscale eddy variability. We find that advective upwelling timescales are much shorter in eddy models than noneddy models with the effect of eddies parameterized by an eddy bolus velocity. These results have important implications for climate projections.

2. Methods

We use the CM2-O suite of atmosphere-ocean general circulation models from the Geophysical Fluid Dynamics Laboratory described extensively in Delworth et al. (2012) and Griffies et al. (2015). The suite consists of models with nominal ocean resolutions of 1° (CM2-1deg), 0.25° (CM2.5), and 0.1° (CM2.6). The atmospheric model, initial conditions, and physics are identical for all three models except for the horizontal resolution in the ocean and the addition of a mesoscale eddy parameterization for CM2-1deg (Griffies et al., 2015). The mesoscale eddy parameterization adds an enhanced isopycnal diffusion and an advection component to the tracer equations in the model. For the coarse-resolution model CM2-1deg, we include the eddy-induced velocities from the eddy parameterization as recommended by Drijfhout et al. (2003). We do not include a parameterization of eddy-induced stochastic forcing for the CM2-1deg trajectories, choosing instead to focus on seawater pathways as defined by the residual mean velocity. Exploration of how best to include such noise-driven diffusion for Lagrangian trajectories remains an ongoing research topic, with recent advances made by Shah et al. (2017) and further reviewed by van Sebille et al. (2018).

Griffies et al. (2015) and Dufour et al. (2015) evaluated elements of the physical integrity for the ocean simulations. Of primary importance for our study is the Southern Ocean residual overturning stream function, which is shown in supporting information Figure S1. The structure of the residual overturning is remarkably similar across the different model configurations, with a range of 15.0–16.8 Sv at 30°S. All of the models are spun up with preindustrial forcing (radiative gases held constant at values for the year 1860) for 181 years at which point we sample 5 day averaged three-dimensional velocity fields during years 182–193.

Lagrangian particles are tracked offline using the Connectivity Modeling System (Paris et al., 2013), a toolbox that uses a Runge-Kutta four-step integration scheme to compute Lagrangian trajectories from model velocity fields. The Connectivity Modeling System has been used to track water mass pathways in various studies, such as Garzoli et al. (2015), van Sebille et al. (2013), and Weijer and van Sebille (2014). The velocities are linearly interpolated in space and time from the model grid to particle positions at every 1 h Lagrangian time step. Since model velocities are only available at 5 day temporal resolution for 12 years and the advective timescales of deep water are known to be on the order of centuries (Khaliwala et al., 2012), we loop over the model output fields as needed.

Lagrangian trajectories are calculated by sampling 5 day averaged velocity fields in each of the three model configurations, with experiments named CM2-1deg-5day, CM2.5-5day, and CM2.6-5day. To isolate the impact

of eddy variability (defined as fluctuations from the 12 year time mean) on upwelling, we analyzed an additional experiment, CM2.6-monthly, where we temporally degrade the CM2.6-5day velocity fields by averaging the velocities over a 1 month period rather than a 5 day period (Qin et al., 2014; Spence et al., 2014 also use monthly means). Spectral analysis shows that removing timescales shorter than 1 month corresponds to decreasing the vertical eddy kinetic energy by about an order of magnitude over length scales of 5–1,000 km, with a peak in the vertical eddy kinetic energy centered near the mesoscale range at 50–200 km (spectral analysis follows Rocha et al., 2016). The vertical eddy kinetic energy wavenumber spectra in CM2.6-monthly are more similar to those of CM2.5-5day than those of CM2.6-5day for all scales from 50 to 1,000 km (see supporting information Text S1 and Figure S2).

In each of the Lagrangian experiments, particles are released on the 15th day of each month for years 183–192 of the first loop. For each release date, particles are released on a 30°S transect of the CM2.6 grid (every 0.1° longitude and on each model depth surface). We track only particles released between depths of 1,000 m and 4,000 m, and we stop tracking them if they cross north of 30°S. This range of release depths is chosen to include densities associated with the upwelling limb of the residual overturning stream function (supporting information Figure S1). Particle trajectories are integrated for 200 years in the CM2.6 experiments, 300 years in the CM2.5 experiment, and 500 years in the CM2-1deg experiment. A particle is considered to have upwelled once it reaches a depth of less than 300 m, a proxy for the depth of the Southern Ocean mixed layer (sensitivity to the definition of the upper ocean boundary is discussed in supporting information Text S2; see also supporting information Figure S3).

For the remainder of the analysis, we consider only the subset of particles that reach the upper ocean south of 30°S within the Lagrangian integration time period (3–5% of the roughly 3 million particles released, depending on the experiment). Most of the particles that do not reach the upper ocean recirculate back across 30°S at depth within the integration time (Tamsitt et al., 2017). Trajectories are no longer tracked once particles reach the upper ocean for the first time, which isolates the upwelling branch of the overturning from subsequent surface water mass transformations and northward return flows. To quantify the transport of deep waters from the deep ocean at 30°S to the upper ocean, each particle is weighted with a fraction of the total southward transport at 30°S at release. The particle's transport is defined by the product of the local instantaneous velocity (interpolated linearly to release position in time and space) with the area of the associated grid face (Blanke et al., 1999; see also Appendix A of Doos et al., 2008). We refer to the sum of transport weights assigned to a set of particles as "particle transport." A natural diagnostic for upwelling Circumpolar Deep Water (CDW) is the sum of the particle transport that is released in the deep ocean at 30°S and reaches the upper layers of the Southern Ocean; we refer to this quantity as Lagrangian Upwelling Transport (LUT). As discussed in supporting information Text S3, we find that uncertainty and error due to the Lagrangian method are negligible for our purposes.

3. Results

We begin with a description of the spatial distribution of particle trajectories between 30°S at depth and the upper layers of the Southern Ocean, defined here as south of 30°S and shallower than 300 m. The time evolution of a subset of particle trajectories in CM2.6-5day, colored by particle depth, is provided in supporting information Movie S1. While these individual particle trajectories are useful for building intuition about the pathways of deep water upwelling, statistical analysis of the entire particle transport data set is required to quantify pathways in terms of volume transport.

Figure 1 shows the percentage of the particle transport that visits each 1° latitude by 1° longitude grid column at least once along trajectories from 30°S to the upper ocean, where darker color signifies that more particle transport passes through the grid column. The relative decrease in color saturation in Figure 1 as resolution increases is due to particle transport completing fewer circumpolar loops and hence visiting fewer grid columns. Following Tamsitt et al. (2017), we categorize the pathways as eastern and western pathways in each of the three major basins: the Atlantic, Indian, and Pacific Oceans. We focus on results from CM2.6-5day because it has the most realistic surface eddy field (standard deviation of dynamic sea level compared to the AVISO satellite product) and stratification (temperature at surface and 730 m depth compared to WOCE climatology) (Griffies et al., 2015). The global LUT of 13.5 Sv is dominated by the pathways in the western Atlantic (5.8 Sv) and western Indian (3.4 Sv), followed by the pathways in the western Pacific (1.7 Sv), eastern Atlantic (1.2 Sv), eastern Pacific (1.0 Sv), and eastern Indian (0.6 Sv); the decomposition of Figure 1 by release section is

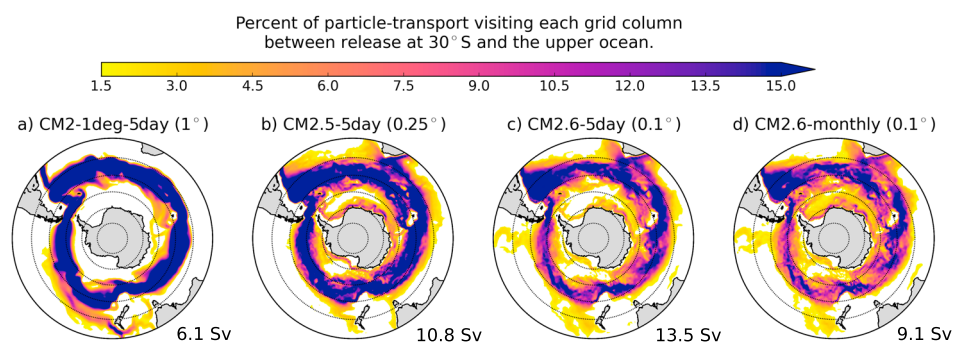


Figure 1. Pathways of CDW from the Lagrangian analyses of (a) CM2-1deg-5day (1°), (b) CM2.5-5day (0.25°), (c) CM2.6-5day (0.1°), and (d) CM2.6-monthly (0.1° , temporally degraded). Colored contours show the percentage of particle transport that visits each 1° latitude by 1° longitude grid column at least once along its trajectory from 30°S to the upper layers of the Southern Ocean. Total particle transport that reaches the upper ocean from 30°S is reported at the bottom right for each experiment.

provided in supporting information Figure S4. The six model pathways southward from 30°S to the Antarctic Circumpolar Current (ACC) in CM2.6-5day are consistent with observations of tracer pathways (Garzoli et al., 2015) and Argo float-derived geostrophic velocities at 1,500 db (Gray & Riser, 2014). In the noneddying experiment CM2-1deg-5day, some of the pathways are vanishingly small, possibly because the pathways do not exist or their timescales are longer than the 500 year integration time.

3.1. Transit Time Distribution for Seawater Particles

The Lagrangian framework naturally allows for estimation of advective timescales for seawater particles. The transit time distribution (TTD) of particle transport is a probability distribution of the time it takes for particle transport to travel from 1,000 to 4,000 m depth at 30°S to the upper ocean. Figure 2a shows the transport-scaled TTD (transparent lines) and smooth inverse Gaussian fits (opaque lines) for each of the experiments (see supporting information Text S4 for a discussion of the fits). Comparing the transport-scaled fitted TTDs between the Lagrangian experiments, we find that horizontal model resolution affects the timescales of upwelling from 30°S to the upper ocean (Figure 2a, black lines). Between the three horizontal ocean resolution experiments CM2-1deg-5day (1°), CM2.5-5day (0.25°), and CM2.6-5day (0.1°), the most probable transit time, or mode, of the transport-scaled fitted TTD decreases from 87 years to 31 years to 17 years, respectively. This transition toward shorter timescales with increased horizontal resolution holds for each of the six individual pathways (supporting information Figures S5a–S5c). The omission of isopycnal diffusion and any differences between the prescribed isopycnal diffusivity in the noneddying model and the effective isopycnal diffusivity in the eddying models may be responsible for differences between the TTDs in noneddying and eddying models, but it is unclear how they would affect the mode of the TTDs. We hypothesize that the increase in eddy variability, realized as the horizontal grid is refined, is partially responsible for the decrease of the Lagrangian upwelling timescale from 1,000 to 4,000 m at 30°S to the upper layers of the Southern Ocean. A dependence on eddy variability is consistent with current dynamical understanding of the Southern Ocean overturning circulation (Marshall & Speer, 2012).

To isolate eddy variability from other potential differences between the three Lagrangian analyses (e.g., atmospheric forcing and topographic resolution), we compute Lagrangian trajectories in the experiment CM2.6-monthly, in which the velocity fields are temporally degraded such that an order of magnitude of vertical and horizontal eddy kinetic energy is removed (see supporting information Text S1 for spectral analysis). As with the horizontal ocean resolution experiments, temporal smoothing of the eddy velocities used in CM2.6-5day (Figure 2a, black solid line) from 5-day averages to monthly averages shifts the TTD mode of CM2.6-monthly (Figure 2a, red solid line) from a mode of 17 years to 26 years. This experiment supports our hypothesis that an increase in eddy variability results in a decrease of the advective CDW upwelling timescale.

The increase in timescale at coarser resolutions or with temporal smoothing partially reflects the reduced LUTs, which are also likely related to the decrease in eddy variability (as also found in Spence et al., 2014). Tamsitt et al. (2017) show that the upward motion of particles upwelling along isopycnals is enhanced in regions where the ACC interacts with bottom topography and eddy kinetic energy is enhanced. Particles in our experiments with lower eddy variability (CM2-1deg-5day and CM2.6-monthly) appear to have reduced connectivity

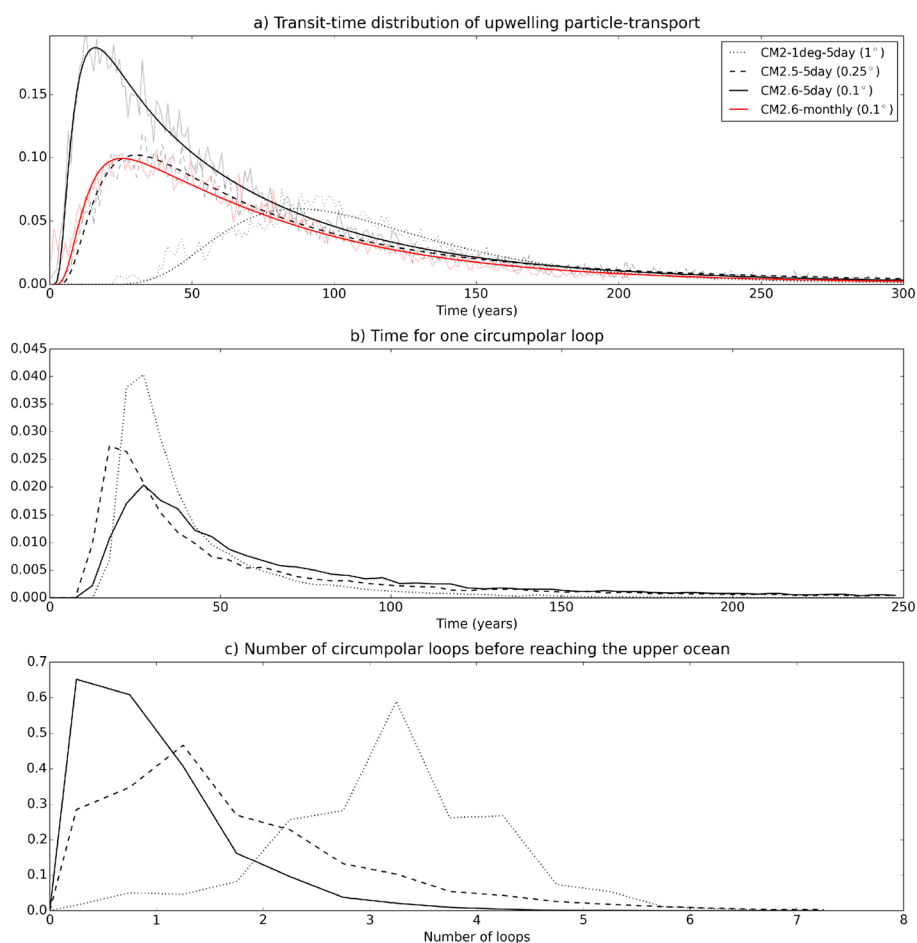


Figure 2. (a) Transit time distributions of particle transport between release at 30°S to the 300 m depth surface in the experiments CM2-1deg-5day (1°), CM2.5-5day (0.25°), CM2.6-5day (0.1°), and CM2.6-monthly (0.1°, temporally degraded). (b) Transport-weighted probability distribution function of the mean time for one particle to complete a circumpolar loop before reaching the upper ocean. (c) Probability distribution function of the number of circumpolar loops completed before reaching the upper ocean. The modes of the TTD distributions and mean number of loops for are, respectively, 87 years and 3.2 loops for CM2-1deg-5day, 31 years and 1.7 loops for CM2.5-5day, 17 years and 0.9 loops for CM2.6-5day, and 26 years and 0.9 loops for CM2.6-monthly.

across the ACC; they exhibit less transport overall, more northerly surfacing locations, and a higher fraction of their transport being laterally advected into deep mixed layers (supporting information Figures S6 and S7). If we approximate the LUT as steady flow with a constant velocity and cross-sectional area, then we find that the reduced LUT in CM2.5-5day and CM2-1deg-5day can explain 30% of the increase in timescales compared with CM2.6-5day (choosing the mode of the TTD as a typical timescale). This simplistic stream tube model of LUT assumes that the TTD is reduced to a delta function. The change in the shape of the TTD between experiments indicates that this simple model is not valid and that the TTD depends on the full spatiotemporal evolution of the distribution of Lagrangian particle transport. Our results thus suggest that changes in LUT and eddy variability contribute to the decrease in upwelling timescales as model resolution is refined.

One consequence of the dependence of the upwelling timescale on model resolution is the degree to which CDW originating from different basins merges in the Southern Ocean. The transit time for particle transport to complete one eastward circumpolar loop around Antarctica changes little between CM2.1deg-5day, CM2.5-5day, and CM2.6-5day (Figure 2b). The average number of circumpolar loops that particle transport completes decreases with increasing horizontal resolution from 3.2 in CM2-1deg-5day to 1.7 in CM2.5-5day to 0.9 in CM2.6-5day with the mode showing a similar pattern. In CM2.6-5day over 75% of particle transport completes fewer than two loops, compared with less than 25% in CM2-1deg-5day. The omission of isopycnal diffusion may be responsible for some of the differences between CM2-1deg-5day and the eddying models.

Since refining horizontal resolution decreases the number of circumpolar loops traveled by particle transport, we expect that models with finer horizontal grid spacing will have less time to diffusively merge contributions of CDW originating from different ocean basins.

3.2. Residual and LUT

We introduce an Eulerian metric, the Residual Upwelling Transport (RUT), and discuss how we expect it to differ from the LUT. We define RUT as the maximum of the upper cell of residual overturning stream function at the Lagrangian release section of 30°S (supporting information Figure S1). Theoretically, the residual overturning stream function calculated from Eulerian mean and eddy velocity fields is equivalent to the Lagrangian overturning stream function calculated from volume-conserving Lagrangian trajectories. Döös et al. (2008) show that this equivalence can be realized in practice with only small errors due to the Lagrangian analysis.

While the zonally integrated RUT is a convenient metric, it is also limited. First, the RUT includes transport pathways that transform diapycnally in the ocean interior so we expect the RUT to be larger than the LUT due to this unventilated upwelling (see interior recirculations in supporting information Figure S1, e.g., the circulation of a few sverdrup at 1,036.5 kg/m³ and 40°S in CM2.5-5day). Second, even for waters that appear to transform diapycnally at the latitude and density of the upper ocean in the residual overturning stream function, they may be artifacts of the time averaging and zonal integration. In contrast, the LUT by definition ensures that only the relevant connected transport of ventilated CDW is taken into account.

We note some challenges in interpreting the LUT for the eddy parameterization experiment (CM2-1deg-5day) and the temporal smoothing experiment (CM2.6-monthly). In CM2-1deg-5day, although the parameterized eddy bolus velocities appear to produce a realistic residual overturning stream function (supporting information Figure S1), it is not clear that their zonal distribution is properly sampled by the three-dimensional Lagrangian upwelling pathways. It is possible that zonal asymmetries in eddy bolus velocities are important for Lagrangian pathways in ways that are not captured by the zonally integrated metrics, such as the RUT. While isopycnal diffusion does not affect RUT, it is possible that its omission in CM2-1deg-5day is partially responsible for the low LUT. In CM2.6-monthly, the temporal smoothing of the velocity field may inhibit the ability for particles to cross fronts of the ACC, as found in Spence et al. (2014), potentially affecting the LUT.

3.3. Synthesis of the Results

We synthesize our results with schematic trajectories of CDW particles as they upwell from 30°S to the upper layers of the Southern Ocean in a noneddy model and in an eddy model (Figure 3a). Isopycnals (blue) in the density ranges of CDW are approximately flat between 30°S and the northern limit of the ACC. Isopycnals slope upward toward Antarctica within the ACC and intersect the base of the upper ocean south of the ACC. Upwelling CDW flows to the surface primarily along these isopycnals (Figure 3b), as demonstrated by the residual overturning stream function (supporting information Figure S1). Particle transport in the noneddy experiment (CM2-1deg-5day, 1°) completes a mean of 3.2 circumpolar loops (magenta line), whereas particle transport in the eddy model (CM2.6-5day, 0.1°) completes a mean of 0.9 loops (yellow-gold line). The time-mean zonal velocities of the two schematic trajectories are similar, as inferred from Figure 2b.

Zonal integration of the circulation (Figure 3b) reveals that while spatial pathways of trajectories appear identical in two-dimensional depth-latitude space, their three-dimensional spatial pathways may differ. Consequently, models with similar residual overturning stream functions (as in supporting information Figure S1) may have completely different timescales (as in Figure 2a). That is, information on how widely the transport is spread out zonally (and hence the average meridional velocity) is lost by the zonal integration. This loss of information is particularly problematic in regions without meridional boundaries, such as the ACC, where meridional transport is not concentrated in boundary currents. Five year intervals are marked along the trajectories by spheres in Figure 3a and circles in Figure 3b, where the transit time is 87 years in CM2-1deg-5day and 17 years in CM2.6-5day.

For the schematic trajectories described above, time-mean Lagrangian meridional and vertical velocities (estimated by mean distance traveled during 5 year intervals) are roughly 5 times greater in the eddy model than in the noneddy model. We hypothesize that increasing eddy variability increases the flow speed of CDW southward and upward along sloping isopycnals in the Southern Ocean, resulting in a shorter upwelling timescale. This result is in agreement with studies showing that beneath the Ekman layer, cross-frontal flow is primarily driven by eddies at and downstream of topography (Dufour et al., 2015) and that high-frequency eddy variability is needed for particles to cross fronts (Spence et al., 2014). Lagrangian analysis by Tamsitt et al. (2017) suggests that the upwelling spiral in the Southern Ocean in eddy models is not as smooth as

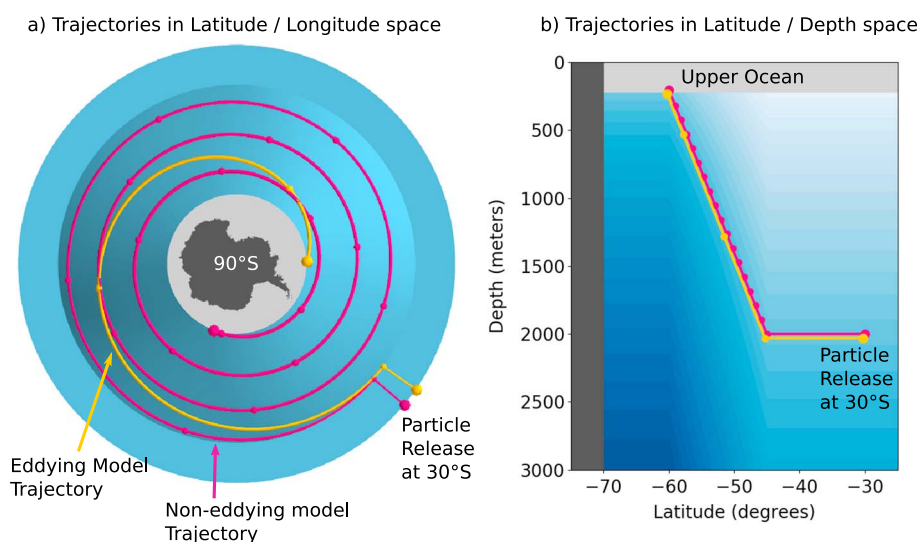


Figure 3. (a) Three-dimensional schematic of CDW upwelling on an isopycnal surface between 30°S and the upper layers of the Southern Ocean. Trajectories of particle transport are shown spiraling eastward, southward, and upward for a noneddying model experiment (CM2-1deg-5day, magenta line) and for an eddying model experiment (CM2.6-5day, orange line). Magenta and orange circles mark 5 year intervals along the trajectories. (b) Projection in depth-latitude of trajectories in Figure 3a with colored density contours overlaid. Lighter shades of blue represent lighter densities.

suggested by our Figure 3a but instead is interrupted by large jumps as particles move southward and upward at eddy hotspots coinciding with major topographic features (see their Figure 4a).

4. Discussion

Quantitative Lagrangian analysis of upwelling pathways in the Southern Ocean reveals that advective timescales for deep waters at 30°S to reach the upper layers of the Southern Ocean decreases from 87 years to 31 years to 17 years as horizontal ocean resolution is refined from 1° to 0.25° to 0.1° (Figure 2). Artificial temporal smoothing of velocity fields in the 0.1° model causes the upwelling timescale to increase from 17 years to 26 years, which suggests that the dependence of the upwelling timescale on model resolution is due to differences in eddy variability. Previous Lagrangian studies of upwelling timescales in the Southern Ocean in time-averaged eddying models and time-dependent noneddying models find relatively long timescales of 140–240 years, consistent with our result that advective upwelling timescales increase as resolution is decreased (Döös, 1995; Iudicone et al., 2008). Neither of these previous estimates include either the advective or diffusive effects of eddies, which may partially explain their relatively long timescales, suggesting the importance of implementing subgrid-scale parameterizations when computing Lagrangian trajectories from noneddying models (Shah et al., 2017; van Sebille et al., 2018). Our results also help to explain the timescale differences reported in Tamsitt et al. (2017), who find shorter timescales in models with higher spatial and temporal resolution, although the models had many other differences besides model resolution. Furthermore, our analysis of a 0.1° resolution model, with a rich eddy field similar to estimates from satellite observations (Griffies et al., 2015), suggests that the real Southern Ocean advective upwelling timescale may be closer to 17 years, up to an order of magnitude shorter than previously reported.

Deep water masses originating in different ocean basins carry varying concentrations of tracers such as carbon, heat, and nutrients to the Southern Ocean, where they mix in the ACC to form CDW. On average, particle transport representing CDW completes fewer circumpolar loops as model resolution is increased, providing the different water masses that constitute CDW less time and distance over which to merge (Figure 2c). The finding that noneddying models overestimate advective Southern Ocean upwelling timescales is potentially important for long-term climate change projections. Armour et al. (2016), for instance, argue that the present-day delayed warming of the Southern Ocean is controlled by the timescale over which heat is advected from North Atlantic Deep Water formation sites to the Southern Ocean upper ocean. Our results suggest that the advective timescales of this warming may be significantly shorter than previously reported.

Mesoscale eddy parameterization efforts generally focus on reconciling zonally integrated meridional transports between noneddying and eddying models (Gent, 2016). Our results suggest that even with very similar residual overturning stream functions, parameterized noneddying models, as well as eddy-permitting models, may be biased toward longer CDW upwelling timescales than eddy active models (Figure 3). Indeed, for applications where connectivity between the deep ocean and the upper ocean is important, the LUT and TTDs may be more meaningful diagnostics than the zonally integrated residual overturning stream function. Future work includes investigating the timescale for tracers to propagate from the North Atlantic to the Southern Ocean and investigating the roles of model resolution and eddy variability on upwelling timescales in both idealized and realistic model configurations.

Acknowledgments

H. F. D. was fully supported by and all other authors (except S. M. G.) were partially supported by Department of Energy's RGCM program through grant DE-SC0012457. J. L. S. and A. R. G. were partially supported by Southern Ocean Carbon and Climate Observation and Modeling through grant PLR-1425989. A. R. G. was supported by the Climate and Global Change Postdoctoral Fellowship from the National Oceanic and Atmospheric Administration. A. K. M. was supported by the Australian Research Council DECRA Fellowship DE170100184. We thank Carolina Dufour, Nathaniel Tarshish, Raffaele Ferrari, and Gregory Wagner for insightful discussion and Mike Winton and John Dunne at GFDL for their support of this project. We also thank the Editor and three anonymous reviewers, whose comments greatly helped clarify our presentation. Code and data are freely available at https://github.com/hdrake/so_lagrangian_upwelling.

References

- Armour, K. C., Marshall, J., Scott, J. R., Donohoe, A., & Newsom, E. R. (2016). Southern Ocean warming delayed by circumpolar upwelling and equatorward transport. *Nature Geoscience*, *9*, 549–554. <https://doi.org/10.1038/ngeo2731>
- Blanke, B., Arhan, M., Madec, G., Roche, S., Blanke, B., Arhan, M., ... Roche, S. (1999). Warm water paths in the equatorial Atlantic as diagnosed with a general circulation model. *Journal of Physical Oceanography*, *29*(11), 2753–2768. [https://doi.org/10.1175/1520-0485\(1999\)029<2753:WWPITE>2.0.CO;2](https://doi.org/10.1175/1520-0485(1999)029<2753:WWPITE>2.0.CO;2)
- Delworth, T. L., Rosati, A., Anderson, W., Adcroft, A. J., Balaji, V., Benson, R., ... Zhang, R. (2012). Simulated climate and climate change in the GFDL CM2.5 high-resolution coupled climate model. *Journal of Climate*, *25*(8), 2755–2781. <https://doi.org/10.1175/JCLI-D-11-00316.1>
- Döös, K. (1995). Interoccean exchange of water masses. *Journal of Geophysical Research*, *100*(C7), 13,499–13,514. <https://doi.org/10.1029/95JC00337>
- Döös, K., Nycander, J., & Coward, A. C. (2008). Lagrangian decomposition of the Deacon Cell. *Journal of Geophysical Research*, *113*, C07028. <https://doi.org/10.1029/2007JC004351>
- Drijfhout, S., de Vries, P., Döös, K., & Coward, A. C. (2003). Impact of eddy-induced transport on the Lagrangian structure of the upper branch of the thermohaline circulation. *Journal of Physical Oceanography*, *33*, 2141–2155. [https://doi.org/10.1175/1520-0485\(2003\)033<2141:IOETOT>2.0.CO;2](https://doi.org/10.1175/1520-0485(2003)033<2141:IOETOT>2.0.CO;2)
- Dufour, C. O., Griffies, S. M., de Souza, G. F., Frenger, I., Morrison, A. K., Palter, J. B., ... Slater, R. D. (2015). Role of mesoscale eddies in cross-frontal transport of heat and biogeochemical tracers in the Southern Ocean. *Journal of Physical Oceanography*, *45*, 3057–3081. <https://doi.org/10.1175/JPO-D-14-0240.1>
- Garzoli, S. L., Dong, S., Fine, R., Meinen, C. S., Perez, R. C., Schmid, C., ... Yao, Q. (2015). The fate of the deep western boundary current in the south atlantic. *Deep-Sea Research Part I: Oceanographic Research Papers*, *103*, 125–136. <https://doi.org/10.1016/j.dsr.2015.05.008>
- Gent, P. R. (2016). Effects of southern hemisphere wind changes on the meridional overturning circulation in ocean models. *Annual Review of Marine Science*, *8*(1), 79–94. <https://doi.org/10.1146/annurev-marine-122414-033929>
- Gray, A. R., & Riser, S. C. (2014). A global analysis of sverdrup balance using absolute geostrophic velocities from Argo. *Journal of Physical Oceanography*, *44*(4), 1213–1229. <https://doi.org/10.1175/JPO-D-12-0206.1>
- Griffes, S. M., Winton, M., Anderson, W. G., Benson, R., Delworth, T. L., Dufour, C. O., ... Zhang, R. (2015). Impacts on ocean heat from transient mesoscale eddies in a hierarchy of climate models. *Journal of Climate*, *28*(3), 952–977. <https://doi.org/10.1175/JCLI-D-14-00353.1>
- Iudicone, D., Speich, S., Madec, G., & Blanke, B. (2008). The global conveyor belt from a Southern Ocean perspective. *Journal of Physical Oceanography*, *38*(7), 1401–1425. <https://doi.org/10.1175/2007JPO3525.1>
- Khatiwala, S., Primeau, F., & Holzer, M. (2012). Ventilation of the deep ocean constrained with tracer observations and implications for radiocarbon estimates of ideal mean age. *Earth and Planetary Science Letters*, *325–326*, 116–125. <https://doi.org/10.1016/j.epsl.2012.01.038>
- Marshall, J., & Speer, K. (2012). Closure of the meridional overturning circulation through Southern Ocean upwelling. *Nature Geoscience*, *5*(3), 171–180. <https://doi.org/10.1038/ngeo1391>
- Morrison, A. K., Frölicher, T. L., & Sarmiento, J. L. (2015). Upwelling in the Southern Ocean. *Physics Today*, *68*(1), 27–32. <https://doi.org/10.1063/PT.3.2654>
- Paris, C. B., Helgers, J., van Sebille, E., & Srinivasan, A. (2013). Connectivity Modeling System: A probabilistic modeling tool for the multi-scale tracking of biotic and abiotic variability in the ocean. *Environmental Modelling and Software*, *42*, 47–54. <https://doi.org/10.1016/j.envsoft.2012.12.006>
- Qin, X., van Sebille, E., & Sen Gupta, A. (2014). Quantification of errors induced by temporal resolution on Lagrangian particles in an eddy-resolving model. *Ocean Modelling*, *76*, 20–30. <https://doi.org/10.1016/j.ocemod.2014.02.002>
- Rocha, C. B., Chereskin, T. K., Gille, S. T., & Menemenlis, D. (2016). Mesoscale to submesoscale wavenumber spectra in drake passage. *Journal of Physical Oceanography*, *46*(2), 601–620. <https://doi.org/10.1175/JPO-D-15-0087.1>
- Shah, S. H. A. M., Primeau, F. W., Deleersnijder, E., & Heemink, A. W. (2017). Tracing the ventilation pathways of the deep North Pacific Ocean using Lagrangian particles and Eulerian tracers. *Journal of Physical Oceanography*, *47*(6), 1261–1280. <https://doi.org/10.1175/JPO-D-16-0098.1>
- Spence, P., van Sebille, E., Saenko, O. a., & England, M. H. (2014). Using eulerian and lagrangian approaches to investigate wind-driven changes in the southern ocean abyssal circulation. *Journal of Physical Oceanography*, *44*(2), 662–675. <https://doi.org/10.1175/JPO-D-13-0108.1>
- Tamsitt, V., Drake, H. F., Morrison, A. K., Talley, L. D., Dufour, C. O., Gray, A. R., ... Weijer, W. (2017). Spiraling pathways of global deep waters to the surface of the Southern Ocean. *Nature Communications*, *8*(1), 172. <https://doi.org/10.1038/s41467-017-00197-0>
- Thompson, A. F., & Sallée, J.-B. (2012). Jets and topography: Jet transitions and the impact on transport in the Antarctic Circumpolar Current. *Journal of Physical Oceanography*, *42*(6), 956–972. <https://doi.org/10.1175/JPO-D-11-0135.1>
- van Sebille, E., Griffies, S. M., Abernathy, R., Adams, T. P., Berloff, P., Biastoch, A., ... Zika, J. D. (2018). Lagrangian ocean analysis: Fundamentals and practices. *Ocean Modelling*, *121*, 49–75. <https://doi.org/10.1016/j.ocemod.2017.11.008>
- van Sebille, E., Spence, P., Mazloff, M. R., England, M. H., Rintoul, S. R., & Saenko, O. A. (2013). Abyssal connections of Antarctic Bottom Water in a Southern Ocean State Estimate. *Geophysical Research Letters*, *40*, 2177–2182. <https://doi.org/10.1002/grl.50483>
- Weijer, W., & van Sebille, E. (2014). Impact of Agulhas Leakage on the Atlantic Overturning Circulation in the CCSM4. *Journal of Climate*, *40*, 1138–1143. <https://doi.org/10.1175/JCLI-D-12-00714.1>